

AD-A099 077

FOREIGN TECHNOLOGY DIV WRIGHT-PATTERSON AFB OH

F/G 20/5

2 KW TRANSVERSE-FLOW CYCLE CO2 LASER, (U)

APR 81 W ZHEEN, S BAORONG, H SHAOYI

UNCLASSIFIED

FTD-ID(RS)T-0108-81

NL

1 OF 1
AD A
099077



END
DATE
FILMED
6-81
DTIC

AD A099077

2

FTD-ID(RS)T-0108-81

FOREIGN TECHNOLOGY DIVISION



2 kW TRANSVERSE-FLOW CYCLE CO₂ LASER

by

Wang Zheen, Su Baorong, et al.

DTIC
ELECTRONIC
MAY 15 1981

B



DTIC FILE COPY

Approved for public release;
distribution unlimited.



01 0 15 151

EDITED TRANSLATION

(1) FTD-ID(RS)T-0108-81 (11) 29 Apr 1981

MICROFICHE NR: FTD-81-C-000363

2 KW TRANSVERSE-FLOW CYCLE LASER

By: Wang Zheer, Su Baorong, Chen Kexin, W. J. Dai, Xi Guoxi

English pages: 9

(2) Edited trans Laser Journal v7 n7 p1-9 1980

Country of origin: (China)
Translated by: SCITRAN
F33657-78-D-0619

Requester: FTD/TQTD
Approved for public release; distribution unlimited.

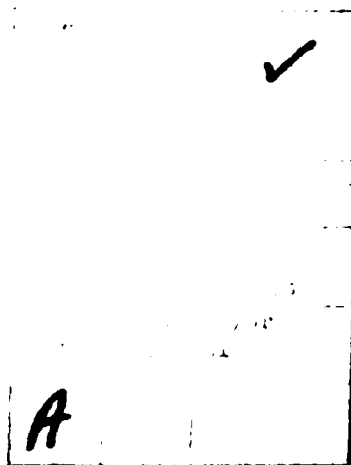
(11)

<p>THIS TRANSLATION IS A RENDITION OF THE ORIGINAL FOREIGN TEXT WITHOUT ANY ANALYTICAL OR EDITORIAL COMMENT. STATEMENTS OR THEORIES ADVOCATED OR IMPLIED ARE THOSE OF THE SOURCE AND DO NOT NECESSARILY REFLECT THE POSITION OR OPINION OF THE FOREIGN TECHNOLOGY DIVISION.</p>	<p>PREPARED BY: TRANSLATION DIVISION FOREIGN TECHNOLOGY DIVISION WP.AFB, OHIO.</p>
---	--

141

2 kW TRANSVERSE-FLOW CLOSED CYCLE CO₂ LASER

Wang Zheen, Su Baorong, Hu Shaoyi, Chen Xexin,
Wu Donglai, Xi Qianxin, Cui Jinsi, Yu Zhiqiang,
and Cheng Zhaogu

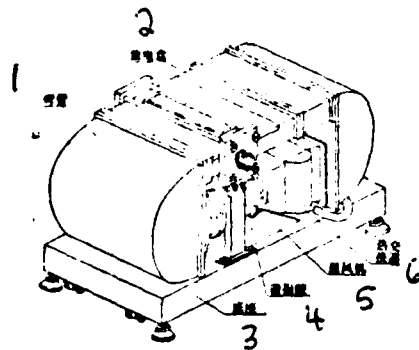


I. Experimental apparatus and characteristics

The transverse-flow CO₂ laser is schematically shown in Figure 1. It consists of an electrical discharge chamber, a pumping system, a heat exchanger, and the return flow pipe. The electrical discharge chamber is rectangular in shape with its throat (height 40 mm) as the discharge and chamber regions. The upstream area is the compressed area while the downstream area is the expansion area. An axial pump is placed in the vacuum system powered by a 400 Hz electric motor. The heat exchanger is designed to have high heat exchange capability, compact structure, light weight and good durability. The cooling power is approximately 10,000 kcal/hour at a cooling water flow rate of 1500 kg/hour. The return flow tube consists mainly of the two semi-circular tubes which connect the discharge chamber, the heat exchanger, and the pump into a closed loop (external dimensions 1.25 m x 2.25 m x 1.25 m). The system uses "O" ring seals and a vacuum of 10⁻¹ mm Hg can be obtained. The volume of the laser is about 1 m³. The volumetric flow rate is 1.3 m³/sec. The working pressure is 46 mm Hg. The working gas consists of CO₂: N₂: He at a ratio of 1:7:14.5. The mass transport rate in is 43 g/sec measured with a pitot tube.

Figure 1. Schematic diagram of a transverse flow CO₂ laser.

1) semi-circular tube; 2) discharge chamber; 3) base; 4) resonance chamber; 5) pump; 6) heat exchanger



The resonance chamber is a single passage chamber 1.25 meter in length. The window is coated with a flat coating of GaAs with

* Paper received October 12, 1979.

a 20% transmittance. The reflective mirror is made of gold coated $\phi 70$ quartz. The radius of curvature is 2.2 meters.

The maximum output of the DC power supply is 50 kW. With an input current of about 12 amperes, the output is about 2 kW. The optical spots at the unit are shown in Figure 2.

Figure 2. Optical spots at the exit at 2 kW

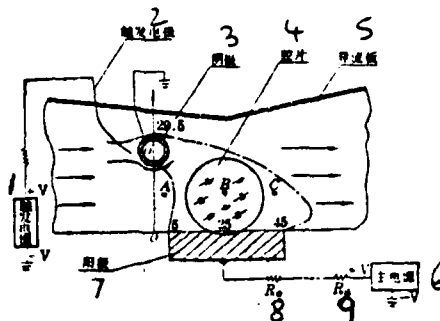


II. Electrode structure

The electrode structure is schematically shown in Figure 3 [1]. The cathode is located upstream near the top of the discharge chamber. The anode is placed downstream from the cathode. The anode is tied to the bottom plate of the discharge chamber, forming the same plane. The rear of the copper tube cathode is lined up with the front of the copper strip anode. A set of triggering pins is evenly placed upstream from the cathode. The actual parameters are as follows:

tubular cathodes: $\phi 10$ water cooled polished copper tube.
strip anodes : 45 copper strips, 15 mm wide and 40 mm long, 4 mm apart and electrically insulated from each other.
triggering electrodes: $\phi 1$ copper wire located upstream of the cathode about 5-6 mm and evenly distributed.
limiting resistors: each anode strip is connected to a proper limiting resistor R_{branch} and then connected to a common resistor R_{total} .
main current I_{main} (2 kW output) 12 ampere
working pressure (46 mm Hg)--1200 volts
triggering current sum 100 mA

Figure 3. Electrode structure



Key: 1) triggering power source; 2) triggering electrode; 3) cathode; 4) chamber plate; 5) conducting plate; 6) main power supply; 7) anode; 8) R_{branch} ; 9) R_{total}

Experimental results indicate that the diameter of the cathode tube directly affects the formation of the arc, the magnitude of the E/p ratio, and the output power. This is due to the fact that the electric field strength near a conductor (area under the cathode) is heavily dependent on the radius r [2]. The smaller r is, the higher the field strength near the conductor which is more advantageous in maintaining the stability of the discharge and reducing the gas resistance. However, we have also to consider that a well defined cathode area is needed in order to ensure electrical power input. The dimensions of the anode strip must be matched with the requirements of the resonance chamber. The filling and spacing must take gas diffusions and heat evolution into consideration [3].

The distance between the anode and the cathode should be carefully selected. The power output is lowered if the distance is too short; on the other hand, the stability is hampered if the distance is too far. Our experimental results showed that the distance should be 29.5 mm for optimal performance (see Figure 3).

III. Discharge and output characteristics

1. The effect of DC power supply on the waveform of the output beam

When the output of a DC power supply contains significant AC components, it means that in addition to the DC excitation an AC component with continuously varying voltage also exists in the excitation. Such an AC component affects the discharge stability and the electricity-to-light conversion efficiency significantly. The effect can be clearly shown in the laser output power level. For example, under fully rectifying and semi-rectifying conditions the former provided an output of 800 watts and the latter only 600 watts at the same 5 ampere input current level.

The elimination of the AC component in the DC power supply, the improvement in the stability of the power supply and the increase in the output level of the power supply are extremely important in the optimization of laser power output.

2. The effect of limiting resistors on the power output and efficiency

In order to simultaneously light up all the anodes, a limiting resistor of a fixed resistance (600 ohm) is required for each electrode. Another common resistance R_{total} must also be connected in series on the return line to the main power supply. Experimental results indicated that the value of R_{total} affects the discharge stability and the laser power output significantly. It becomes more pronounced with increasing current. In order to ensure stability under large current discharge conditions, R_{total} should be not less than 250 ohm (see Figure 1).

TABLE 1. The effect of R_{total} on the stability of discharge and laser power output

|| ($I_{in}=9$ 安培, $I_{out}=110$ 毫安, 工作气压为46毫米汞柱)

1 I_{in} (安培)	0	95	130	180	240	260	300
2 P_L (瓦)	30	1460	1590	1700	1760	1760	1736
3 放电稳定性	4 放电极不稳, 无弧	5 放电不稳, 有弧	6 放电稍稳, 有弧	7 较稳, 无弧	8 稳, 无弧	9 稳, 无弧	10 稳, 无弧

(Key on next page.)

Key to Table 1: 1) R_{total} (ohm); 2) P_{\perp} (watt); 3) discharge stability; 4) not stable, no arc; 5) not stable, arc; 6) slightly more stable, arc; 7) slightly more stable, no arc; 8) stable, no arc; 9) stable, no arc; 10) stable, no arc; 11) ($I_{main}=9$ ampere, $I_{trigger}=110$ mA, working pressure=46 mm Hg)

3. The effect of triggering current

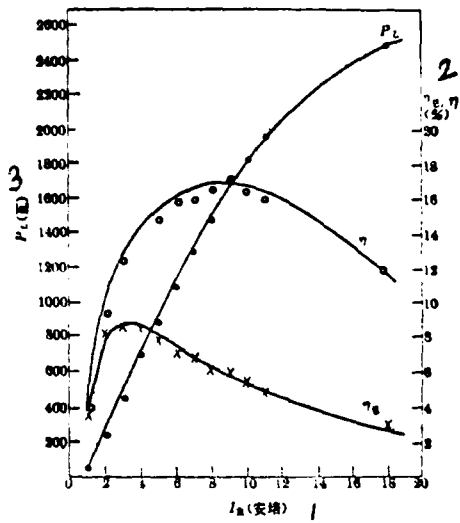
The triggering electrodes are placed upstream of the cathodes. When the working pressure is at 40 mm Hg, the triggering mechanism does not function. The penetrating voltage of the main power supply is 2.4 kV without the triggering system. With a tiny triggering current, the penetrating voltage drops to 1.1 kV (similar to the maintaining voltage). When the pressure increased to 46 mm Hg, the laser would not light up without triggering.

We used a multi-pin triggering mechanism powered by an external DC power supply at a current level of about 100 mA. This arrangement makes it possible to improve the discharge stability when larger main discharge current (above 10 ampere) is used.

It is interesting to point out that the effect of the magnitude of the triggering current on the laser power output is rather insignificant when the main DC power supply delivers good DC signals. However, it becomes extremely important if the DC signal from the main power supply is rather poor (see Figure 5). We concluded that the larger triggering current formed an electronic current which might have compensated the effect of the pulsing DC power supply in the latter case.

4. The effect of working pressure on discharge stability and power output

Since the possible injection electric power and the output laser power are all proportional to the mass transport rate m ,



1. I_{main} (ampere)
2. P_L (watt)
3. η_{total} (%)

Figure 4. The variation of power output P_L , efficiency η and η_{total} as a function of I_{main} ($I_{\text{triggering}}=100 \text{ mA}$)

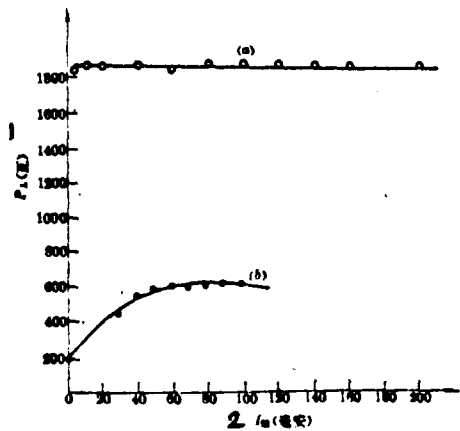


Figure 5. The effect of $I_{\text{triggering}}$ on the power output P_L
 Key: 1. P_L (watt)
 2. $I_{\text{triggering}}$ (Ma)

- (a) good DC power supply
 $I_{\text{main}}=9.5 \text{ ampere}$
 $P=46 \text{ torr.}$
 (b) poor DC power supply
 $I_{\text{main}}=5 \text{ amp}$
 $P=35 \text{ torr}$

TABLE 2. Laser power P_L , discharge stability and pressure. ($\text{Co}_2:\text{N}_2:\text{He}=1:7:14.5$; $I_{\text{trigger}}=100 \text{ mA}$; $R_{\text{total}}=400 \text{ ohm}$, $R_{\text{branch}}=600 \text{ ohm}$, $I_{\text{main}}=10.5 \text{ amp}$).

1 气压 P (毫米汞柱)	47.7	47	46	44	42	40	35	30	20
2 P_L (瓦)	2090	2073	2040	2023	1854	1686	1484	1230	674
3 有无强光	4 弱起强	5 无强	6 无强	7 无强	8 无强	9 无强	10 无强	11 有强	12 有强

(Key on next page.)

Key to Table 2: 1) pressure p (mm Hg); 2) P_L (watt); 3) arc or no arc; 4) easily arc; 5) no arc; 6) no arc; 7) no arc; 8) no arc; 9) no arc; 10) no arc; 11) arc; 12) arc

the working pressure p must be raised in order to increase the power level. However, it is more difficult to light up the laser when the pressure is too high. Arcing is usually occurring. In order to improve the discharge, we adopted a proper mixture with larger He content ($\text{CO}_2:\text{N}_2:\text{He}=1:7:14.5$) and operated at a working pressure of 46 mm Hg.

Experimental results showed that under no arcing conditions the output power level increases linearly with the pressure at the same main input current value. When the pressure dropped to 30 or 20 mm Hg, arcing occurred because the mass transport rate was drastically decreased while the input current still remained at 10.5 ampere.

5. Localized effect due to non-uniform electric field strength, the selection of chamber position and transmittance of the window

Due to the fact that the surface of a conductor is always at the same potential, the electric field E at any point then is directed perpendicular to the surface of the conductor. Considering that charge density in the ionization region is zero and neglecting the variation of electric field strength due to wind speed [2], the electric field E in the laser discharge region can be approximated using a mirror-image method. The current source can be treated as if it existed in the center axis of the tubular cathode. Apparently, both positive and negative charges would migrate towards region D of the cathode and region F on the anode (see Figure 3). Calculation indicates the E/P values at points A (coordinates 5, 15), B(coordinates 25, 15) and C (coordinates 45, 15) differ significantly. Assuming the electric field at point A is E_A , then $E_B \approx 3E_A/11$ and $E_C \approx E_A/11$. It is easy to figure out that

the E/P value at point A is about 8.7 V/cm-torr which is almost ideal for the selective excitation of N_2 and CO_2 . At point B (approximately at the center of the resonance chamber) and point C (further downstream) the E/P values are significantly less. Consequently, the current density n_0 is lowered. On the other hand, the relaxation time of CO_2 molecules in the excited states is about 1 msec [5]. The flow speed in the discharge region is about 4×10^3 cm/sec. Therefore, some of the excited molecules not involved in the laser process may drift downstream by 4 cm, which effectively enlarges the distribution of the excited molecules to a larger region downstream. Due to molecular heat dissipation effect excited molecules can reach the upstream of the lasing region also, contributing to the laser power output. Despite the nonuniform distribution of these benefits, the output beam still remains pretty much uniform since the magnitude of these beneficial effects are dependent upon the light intensity (saturation effect) and the reaction of the resonance chamber (common half focus chamber) effect (see Figure 2).

We used a single path resonance chamber to deliver the laser power. Experiments showed that the axis of the resonance chamber should be placed in the middle (or slightly lower toward the anode) between the axis of the tubular cathode and the bottom plate as indicated in Figure 3 as the 0'0 line. It was found that the horizontal position of the resonance chamber should be placed in the middle of the anode strips or at about 3 mm upstream for best results. The former provided a longer light spot in the horizontal position. Figure 4 showed the results obtained at 3 mm upstream with the light spots shown in Figure 2.

A transverse-flow CO_2 laser, despite its higher power output level, does not have significantly higher beneficial effects over a diffusion type longitudinal CO_2 laser. Its saturation parameter, however, is considerably larger, especially using a single path resonance chamber. The transmittance of the window should be kept

low. In our experiments, transmittance at 10.5 appeared to be the best.

REFERENCES

- [1] Theodore S. Fabian; *IEEE J. Quant. Electr.*, QE-11(1975), 848.
- [2] П. И. Безмястнов и др.; «Газовые лазеры», Новосибирск, «Наука», 1977.
- [3] A. E. Hill; AIAA Paper, No. 71-65.
- [4] 曹昌祺; «电动力学», 1962年版, p87.
- [5] Russell Targ *et al.*; *Appl. Phys. Lett.*, 9(1965), 302.
- [6] 朱如曾, 封开印编译, «激光物理», 1975年版, p57.
- [7] 秋业松光(秋); «レーザー研究», 1976, 4, No. 3, 242~248.

Key: [4] Tso Chan Chi; "Electrodynamics", 1962; p. 87
[6] Chu Ru Tseng, "Laser Physics", 1975, p. 57
[7] Akinari Toshimitsu *et al.*; "Laser Research", 1976, 4, Nr. 3, 242-248.

Abstract

The combination of a closed-cycle, transverse-flow 2KW CW CO₂ laser is described with emphasis on the arcless electrode construction and glow discharge characteristics. By means of a multi-pin trigger, the glow discharge stability is appreciably increased at more intense input current. The direct current output characteristics of the main supply and the selection of the ballast resistor greatly affect the glow discharge stability and the output power.

When the gas flow velocity in the discharge region is 40 m/s, the gas mixture pressure is 46 mmHg, the length of active region is 86 cm, a CW multimode output power of more than 2 KW and an electro-optic efficiency of about 15% are achieved.

DATE
FILMED
-18